

# The “Picrate Effect” on Extraction Selectivities of Aromatic Group-Containing Crown Ethers for Alkali Metal Cations<sup>1</sup>

Galina G. Talanova,<sup>\*,†</sup> Nazar S. A. Elkarim,<sup>†</sup> Vladimir S. Talanov,<sup>†</sup> Robert E. Hanes, Jr.,<sup>†</sup> Hong-Sik Hwang,<sup>†</sup> Richard A. Bartsch,<sup>\*,†</sup> and Robin D. Rogers<sup>\*,‡</sup>

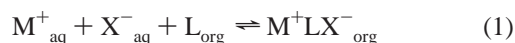
Contribution from the Department of Chemistry and Biochemistry, Texas Tech University, Lubbock, Texas 79409-1061, and the Department of Chemistry, The University of Alabama, Tuscaloosa, Alabama 35487-0336

Received May 12, 1999. Revised Manuscript Received October 23, 1999

**Abstract:** As evaluated with 15 crown ethers which contain varying numbers of benzo substituents, the magnitude of the extraction selectivities (and in one case, the selectivity order) of aromatic group-containing ionophores for alkali metal picrates may vary significantly from those for alkali metal salts with inorganic anions as a result of  $\pi$ – $\pi$  interactions between picrate ion and an aromatic unit of the ionophore. The importance of the “picrate effect” increases as the number of benzo groups in the crown ether is enhanced and varies with their location in the macrocycle. To verify the involvement of picrate–crown ether  $\pi$ -stacking in complexation, crown ether–alkali metal picrate complexes were examined in solution by <sup>1</sup>H NMR spectroscopy and solid-state structures for nine complexes were determined by X-ray diffraction. Dependence of the chemical shift for the picrate proton singlet in the NMR spectrum on the metal cation and/or macrocycle identity in the metal picrate–crown ether complex was found to be a convenient tool for studying anion–ligand  $\pi$ – $\pi$  interactions in solution.

## Introduction

For more than three decades since the initial report of crown ethers (CEs),<sup>2</sup> these macrocyclic compounds, known for their unique capability to selectively complex alkali metal cations, have been intensively investigated as complexing agents in metal ion separations by solvent extraction, membrane transport, and sorption.<sup>3</sup> In such processes, alkali metal salts are transferred from aqueous solution into the hydrophobic organic phase due to formation of ion pair complexes with the macrocyclic polyether carriers. The complexation reaction most often proceeds in accordance with eq 1 to yield complexes with a 1:1 metal-to-ligand stoichiometry:



where subscripts aq and org denote species in the aqueous and organic phases, respectively. The stability of the thus formed ion-pair complex controls the efficiency of the metal ion interfacial transfer. In two-phase liquid–liquid systems, the complex stability is defined by the extraction constant,  $K_{ex}$ :

$$K_{ex} = [M^+LX^-_{org}]/[M^+_{aq}][L_{org}][X^-_{aq}] \quad (2)$$

Differences in the  $K_{ex}$  values for CE-alkali metal cation binding determines the selectivity of the macrocyclic ligand in metal ion separations.

The effectiveness of metal ion transfer from aqueous solution into the organic phase not only depends on the cation type and

properties of the ionophore, but also may be influenced strongly by properties of the anion.<sup>4</sup>

Since the early studies of complexing abilities of the CEs toward metal cations,<sup>5a,b</sup> alkali metal picrates (MPic) have been employed frequently to estimate the efficiencies and selectivities of new macrocyclic ionophores in metal ion separations. Soft, polarizable, weakly hydrated Pic<sup>−</sup> is a convenient counterion that provides greater distribution ratios/membrane transport rates for metal ions than do inorganic anions, such as halide, NO<sub>3</sub><sup>−</sup>, ClO<sub>4</sub><sup>−</sup>, and SCN<sup>−</sup>. In addition, Pic<sup>−</sup> is brightly colored which allows for spectrophotometric determination of concentrations of the otherwise “invisible” alkali metal cations. Since the UV spectrum of Pic<sup>−</sup> changes on interaction of metal picrates with macrocyclic ligands due to separation of the ion pairs M<sup>+</sup>Pic<sup>−</sup>,

(3) Izatt, R. M.; Pawlak, K.; Bradshaw, J. S.; Bruening, R. L. *Chem. Rev.* **1995**, *95*, 2529–2586. *Macrocyclic Compounds in Analytical Chemistry*; Zolotov, Yu. A., Ed.; Wiley: New York, 1997. Moyer, B. In *Comprehensive Supramolecular Chemistry*; Gokel, G. W., Ed.; Pergamon: New York, 1996; Vol. 1, pp 377–416. De Jong, F.; Visser, H. C. In *Comprehensive Supramolecular Chemistry*; Reinhoudt, D. N., Ed.; Pergamon: New York, 1996; Vol. 10, pp 13–52.

(4) (a) Olsher, U.; Hankins, M. G.; Kim, D. Y.; Bartsch, R. A. *J. Am. Chem. Soc.* **1993**, *115*, 3370–3371. Lamb, J. D.; Christensen, J. J.; Izatt, S. R.; Bedke, K.; Astin, M. S.; Izatt, R. M. *J. Am. Chem. Soc.* **1980**, *102*, 3399–3403. Yakshin, V. V.; Abashkin, V. M.; Laskorin, B. N. *Dokl. Akad. Nauk SSSR* **1980**, *252*, 239–241 (Eng). Talanova, G. G.; Yatsimirskii, K. B.; Zicmanis, A. H. *Dokl. Akad. Nauk SSSR* **1991**, *319*, 213–215 (English). Inglesias, R.; Dassie, S. A.; Yudi, L. M.; Baruzzi, A. M. *Anal. Sci.* **1998**, *14*, 231–236. (b) Yatsimirskii, K. B.; Talanova, G. G. *Dokl. Akad. Nauk SSSR* **1983**, *273*, 414–416 (English).

(5) (a) Application of the picrate extraction method for evaluating CE complexing abilities was first reported in the following: Frensdorff, H. K. *J. Am. Chem. Soc.* **1971**, *93*, 4684–4688. (b) Based on Frensdorff’s picrate extraction procedure, Cram and co-workers (Koenig, K. E.; Lein, G. M.; Stuckler, P.; Kaneda, T.; Cram, D. J. *J. Am. Chem. Soc.* **1979**, *101*, 3556–3566) suggested a method for the determination of the complex formation constants. (c) This approach was introduced in the following: Bourgoin, M.; Wong, K. H.; Hui, J. Y.; Smid J. *J. Am. Chem. Soc.* **1975**, *97*, 3462–3467.

\* To whom correspondence should be addressed.

† Texas Tech University.

‡ The University of Alabama.

(1) The results of this research were presented in part at the 216th National Meeting of the American Chemical Society, Boston, MA, August 23–27, 1998, INOR 8.

(2) Pedersen, C. J. *J. Am. Chem. Soc.* **1967**, *89*, 7017–7036.

picrates may be used to determine the complex formation constants in solution.<sup>5c</sup>

However, structural peculiarities of  $\text{Pic}^-$  produce special properties, such as coordination versatility<sup>6,7</sup> toward metal cations, surface activity,<sup>8</sup> and the capability of  $\pi$ - $\pi$  interactions<sup>7,8</sup> between  $\text{Pic}^-$  and aromatic groups of the ionophores. As discussed elsewhere,<sup>7</sup>  $\pi$ -stacking in metal picrate complexes may either facilitate or retard coordination bonding. These features may cause unexpected complications in the estimation of metal ion separation propensities of the macrocyclic ligands.

In several earlier publications,<sup>4b,7,9</sup>  $\pi$ - $\pi$  interactions of  $\text{Pic}^-$  with aromatic groups of the ligand have been reported in crystal structures of some metal picrate complexes with CEs, calixarenes, and other macrocyclic ligands or assumed in solutions of the complexes based on their NMR and UV spectral characteristics.  $\text{Pic}^-$  was found to be capable of  $\pi$ -stacking with aromatic units of a metal-complexed ionophore even in the absence of anion-cation coordination.<sup>9b</sup> Although a possible influence of  $\pi$ - $\pi$  interactions of  $\text{Pic}^-$  with aromatic groups of macrocyclic ligands upon metal picrate extraction has been suggested in some instances, a definitive demonstration of such a "picrate effect" is lacking.

To the best of our knowledge, the effect of  $\text{Pic}^-$  on the selectivity of aromatic group-containing macrocyclic ligands in metal cation interfacial separations has not been evaluated. For this reason, potential anion-ligand  $\pi$ - $\pi$  interactions are usually ignored in the assessment of metal ion separation properties of ionophores by the widely applied, traditional, picrate extraction method.

If picrate-ligand  $\pi$ - $\pi$  interactions in the MPic-CE complex formed in a liquid-liquid extraction system were important, they would contribute significantly to the overall stability of the ion pair complex  $\text{M}^+\text{LPic}^-$  in the organic phase and thereby influence  $K_{\text{ex}}$ . The occurrence and strength of  $\pi$ -stacking between  $\text{Pic}^-$  and an aromatic unit of the macrocyclic ligand would be controlled by the geometry of the complex cation  $\text{M}^+\text{L}$ , which may vary as the metal ion is changed. Therefore additional stabilization of  $\text{M}^+\text{LPic}^-$  ion pairs due to specific anion-ligand interactions is expected to vary as the alkali metal cation is changed. This would mean that metal ion differentiation by the ionophore with  $\text{Pic}^-$  as the counterion might deviate substantially from that obtained with other anions that are incapable of interacting with the ligand. Therefore, the selectivities of aromatic-substituted macrocyclic ligands for extraction of metal picrates may differ significantly from those for metal halides, nitrates, etc., which would restrict the applicability of picrate extraction results to real-world metal ion separation systems.

(6) Olsher, U.; Feinberg, H.; Frolow, F.; Shoham, G. *Pure Appl. Chem.* **1996**, *68*, 1195–1199.

(7) Harrowfield, J. J. *Chem. Soc., Dalton Trans.* **1996**, 3165–3171.

(8) Muzet, N.; Engler, E.; Wipff, G. *J. Phys. Chem.* **1998**, *102*, 10772–10788. Varnek, A.; Wipff, G. *J. Comput. Chem.* **1996**, *17*, 1520–1531. Varnek, A.; Troxler, L.; Wipff, G. *Chem. Eur. J.* **1997**, *3*, 552–560.

(9) (a) Bell, T. W.; Cragg, P. J.; Drew, M. G. B.; Firestone, A.; Kwok, D.-I. A. *Angew. Chem., Int. Ed. Engl.* **1992**, *31*, 345–347. Hughes D. L.; Wingfield, J. N. *Chem. Commun.* **1977**, 804–805. Bhagwat, V. W.; Manohar, H.; Poonia, N. S. *Inorg. Nucl. Chem. Lett.* **1980**, *16*, 289–292. Hanson, I. R.; Owen, J. D.; Truter, M. R. *J. Chem. Soc., Perkin Trans. 2* **1981**, 1606–1615. Harrowfield, J. M.; Mocerino, M.; Peachey, B. J.; Skelton, B. W.; White, A. H. *J. Chem. Soc., Dalton Trans.* **1996**, 1687–1699. Talanova, G. G.; Yatsimirskii, K. B.; Podgorny, A. V.; Zazorina, V. A. *Zh. Obshch. Khim.* **1990**, *61*, 2042–2047 (Eng). (b) Beer, P. D.; Drew, M. G. B.; Grieve, A.; Ogdan, M. I. *J. Chem. Soc., Dalton Trans.* **1995**, 3455–3465. (c) Doughty, S. M.; Stoddart, J. F.; Colquhoun, H. M.; Slawin, A. M. Z.; Williams, D. J. *Polyhedron* **1985**, *4*, 567–575. Abidi, R.; Asfari, Z.; Harrowfield, J. M.; Sobolev, A. N.; Vicens, J. *Aust. J. Chem.* **1996**, *49*, 183–188.

The goals of this research are to evaluate the ability of  $\text{Pic}^-$  to affect the extraction selectivities of aromatic group-containing CEs for alkali metal cations and to probe for a potential "picrate effect" being produced by  $\pi$ - $\pi$  interactions between  $\text{Pic}^-$  and aromatic group(s) of the macrocyclic polyether ligand.

Herein we report results obtained from competitive extractions of five alkali metal cations ( $\text{Li}^+$ ,  $\text{Na}^+$ ,  $\text{K}^+$ ,  $\text{Rb}^+$ , and  $\text{Cs}^+$ ) from aqueous  $\text{Pic}^-$  and  $\text{I}^-$  solutions<sup>10</sup> into chloroform by a variety of CEs (Figure 1) in which both the ring size and number of benzo substituents are systematically varied. In addition, structural studies of alkali metal picrate-CE complexes in solution and in the solid state are utilized to probe the importance of  $\pi$ - $\pi$  interactions between  $\text{Pic}^-$  and aromatic groups of the ionophore.

## Results and Discussion

**Competitive Extractions of Alkali Metal Picrates and Iodides by Benzo Group-Containing CEs.** The selectivity of an ionophore for different metal cations in a solvent extraction process is characterized by the separation factor,  $\alpha_{\text{M}_1, \text{M}_2}$ ,<sup>11</sup> determined by:

$$\alpha_{\text{M}_1, \text{M}_2} = D_{\text{M}_1}/D_{\text{M}_2} \quad (3)$$

where  $D_{\text{M}_1}$  and  $D_{\text{M}_2}$  are the distribution ratios for competing metal ions,  $\text{M}_1^+$  and  $\text{M}_2^+$ , respectively, between the organic and aqueous phases. The distribution ratio,  $D_{\text{M}}$ , is calculated by:

$$D_{\text{M}} = [\text{MLX}]_{\text{org}}/[\text{M}^+]_{\text{aq}} \quad (4)$$

As is obvious from eqs 2–4, the larger the  $K_{\text{ex}}$  value for  $\text{M}_1^+$  extraction relative to that for  $\text{M}_2^+$  the greater is the  $\alpha_{\text{M}_1, \text{M}_2}$  value and the higher is the selectivity of the CE for  $\text{M}_1^+$  over  $\text{M}_2^+$ .

Extraction selectivity of the CE for metal salts with anions that are incapable of interacting with the ionophore will be independent of the anion identity. In such case, a plot of  $\alpha_{\text{M}_1, \text{M}_2}$  determined for anion  $\text{X}_a^-$  versus  $\alpha_{\text{M}_1, \text{M}_2}$  for anion  $\text{X}_b^-$  will be linear with a slope of 1. (The detailed explanation of such anticipated linearity is provided in the Supporting Information.) Deviation from this line would indicate the presence of anion-ionophore interaction in one of the extraction systems. This approach is applied to probe for the involvement of  $\text{Pic}^-$ -CE interactions in competitive extractions of alkali metal picrates and iodides by ionophores **1–13** (Figure 2). (Individual  $\alpha_{\text{M}_1, \text{M}_2}$  values for picrate and iodide extractions with **1–13** are listed in Tables 19S and 20S, respectively, of the Supporting Information.)

For competitive extractions of  $\text{Li}^+$ ,  $\text{Na}^+$ ,  $\text{K}^+$ ,  $\text{Rb}^+$ , and  $\text{Cs}^+$  from aqueous  $\text{Pic}^-$  and  $\text{I}^-$  solutions by the CEs, the concentrations of lithium salts extracted into the organic phase were too small for accurate determination of the corresponding separation factors  $\alpha_{\text{M}, \text{Li}}$ . Therefore, the possibility of a "picrate effect" on  $\text{Li}^+$  extraction with benzo group-containing CEs will not be discussed in this paper.

**(a) Extractions by 18-Membered CEs.** Five CEs with 18-crown-6 rings and varying numbers of benzo groups, e.g., benzo-18-crown-6 (B18C6, **1**), two positional isomers of dibenzo-18-crown-6 (DB18C6, **4**, and *unsym*-DB18C6, **2**), symmetrical

(10) For this study,  $\text{I}^-$  was chosen for comparison with  $\text{Pic}^-$  since the hydration enthalpy value of  $\text{I}^-$  is close to that of  $\text{Pic}^-$ , but the structure of  $\text{I}^-$  should not promote its interaction with aromatic substituents of the ionophores.

(11) Rice, N. M.; Irving, H. M. N. H.; Leonard, M. A. *Pure Appl. Chem.* **1993**, *65*, 2373–2396.

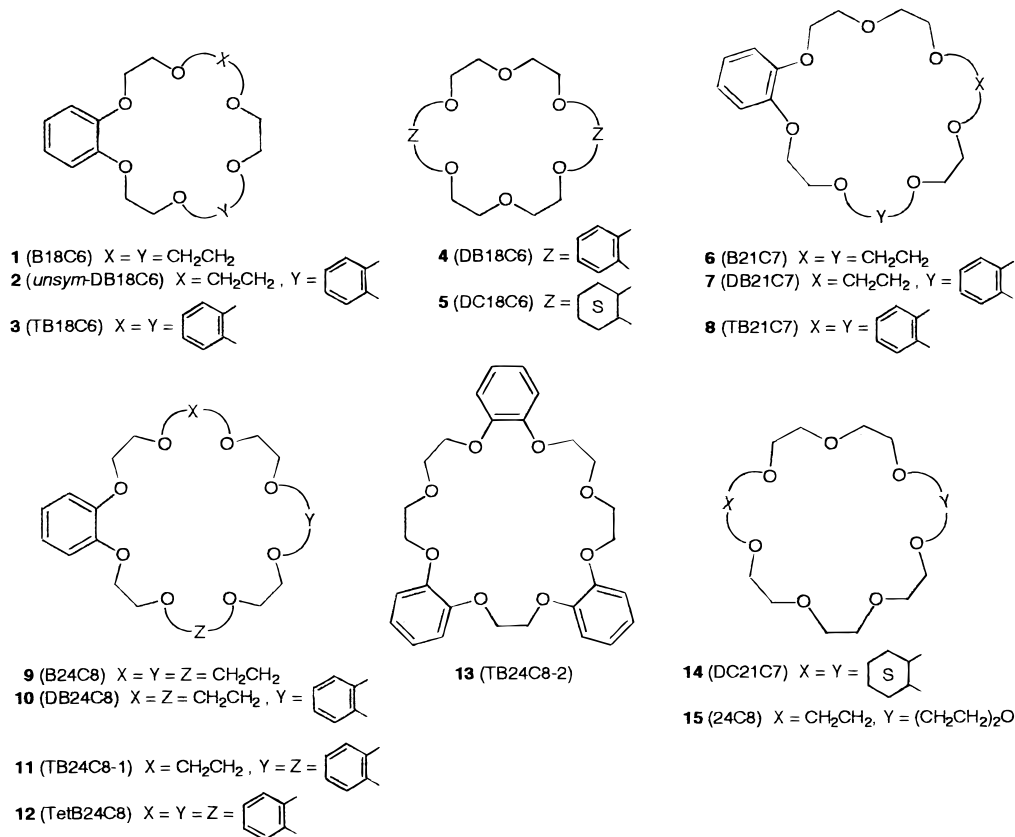


**Figure 1.** Structural formulas of the benzo group-containing CEs and related ligands containing no aromatic moieties.

tribenzo-18-crown-6 (TB18C6, **3**), and also dicyclohexano-18-crown-6 (DC18C6, **5**) that has no aromatic units in the macrocycle, were studied in competitive alkali metal cation extractions. Several of these ionophores are commercially available, K<sup>+</sup>-selective complexants that are frequently employed in metal ion separation studies.

As expected, preferential K<sup>+</sup> transfer from aqueous solution into the organic phase was observed for the competitive alkali metal cation extractions by CEs **1–5** with both Pic<sup>-</sup> and I<sup>-</sup> as the aqueous phase anion. However, as shown in Figure 2a, the separation factors for these CEs, α<sub>K,M</sub>, which determine the efficiency of the K<sup>+</sup> separations from other alkali metal cations, respond differently to the change of counterion from I<sup>-</sup> to Pic<sup>-</sup>.

For the competitive alkali metal extractions by DC18C6 (**5**) that contains no aromatic units, the separation factors were essentially invariant for this change of anion. Thus, the plot of (α<sub>K,M</sub>)<sub>Pic</sub> vs (α<sub>K,M</sub>)<sub>I</sub> for this CE follows the solid line and has a slope of 0.96. For B18C6 (**1**), which contains a single benzo group, only a small deviation from the solid line of unit slope is observed.

In contrast, the α<sub>K,M</sub> values for alkali metal cation extractions with DB18C6 (**4**) and *unsym*-DB18C6 (**2**) vary more significantly with the change of anion. The slope values of the corresponding linear graphs in Figure 2a are 0.58 and 1.46, respectively. Therefore, Pic<sup>-</sup>-CE interactions are involved in alkali metal picrate extractions by both of these ligands. Moreover, the two isomeric CEs, **2** and **4**, show opposite changes in the K<sup>+</sup>/M<sup>+</sup> selectivities when the anion identity was altered. Thus, for the extractions by **2**, (α<sub>K,M</sub>)<sub>Pic</sub> > (α<sub>K,M</sub>)<sub>I</sub>, whereas, for **4**, (α<sub>K,M</sub>)<sub>Pic</sub> < (α<sub>K,M</sub>)<sub>I</sub>. In other words, the selectivity of *unsym*-DB18C6 for K<sup>+</sup> over the other alkali metal cations is enhanced when the aqueous phase anion is changed from I<sup>-</sup> to Pic<sup>-</sup>, while that of DB18C6 is diminished.

With the introduction of a third benzo group in TB18C6 (**3**), the changes in extraction selectivities on going from alkali metal iodides to picrates are even more dramatic than those for the dibenzo-CEs. TB18C6 exhibits almost no differentiation among K<sup>+</sup>, Rb<sup>+</sup>, and Cs<sup>+</sup> in competitive extractions of alkali metal iodides (the separation factors α<sub>K,Na</sub>, α<sub>K,Rb</sub>, and α<sub>K,Cs</sub> were 10.5, 0.95, and 0.93, respectively). However, for extractions of alkali metal picrates by this ligand, α<sub>K,Na</sub>, α<sub>K,Rb</sub>, and α<sub>K,Cs</sub> are 12.1, 4.48, and 11.0, respectively.<sup>12</sup> Therefore, an appreciable selectivity for K<sup>+</sup> over Rb<sup>+</sup> and Cs<sup>+</sup> is observed. In contrast with the graphs of (α<sub>K,M</sub>)<sub>Pic</sub> vs (α<sub>K,M</sub>)<sub>I</sub> for **1**, **2**, **4**, and **5**, an analogous plot for **3** is nonlinear and, therefore, is not shown in Figure 2a.

Thus, Pic<sup>-</sup> has been found to be capable of altering the relative selectivity of alkali metal cation extraction with 18-membered CEs containing benzo groups with the importance of the "picrate effect" increasing with the number of benzo groups in the CE and varying with the location of these aromatic substituents in the macrocyclic polyether ligand.

**(b) Extractions by 21-Membered CEs.** Macrocyclic ligands **6–8**, with 21-crown-7 rings and one to three benzo groups, respectively, were examined in competitive extractions of alkali metal picrates and iodides. In agreement with the previously published data,<sup>13,14</sup> increasing the number of benzo groups in a

(12) It should be noted that a limited solubility of the K<sup>+</sup>(**3**)Pic<sup>-</sup> complex in chloroform resulted in its selective partial precipitation from the organic extract after equilibrium was reached and the phases had been separated (see Experimental Section). For this reason, the (α<sub>K,M</sub>)<sub>Pic</sub> values for **3** given above were calculated based only upon concentrations of alkali metal ions remaining in the organic solution, without consideration of the KPic content in the precipitate.

(13) Talanova, G. G.; Elkarim, N. S. A.; Hanes, R. E.; Hwang, H.-S.; Rogers, R. D.; Bartsch, R. A. *Anal. Chem.* **1999**, *71*, 672–677.

(14) Sachleben, R. A.; Deng, Y.; Bailey, D. R.; Moyer, B. A. *Solvent Extr. Ion Exch.* **1996**, *14*, 995–1015.

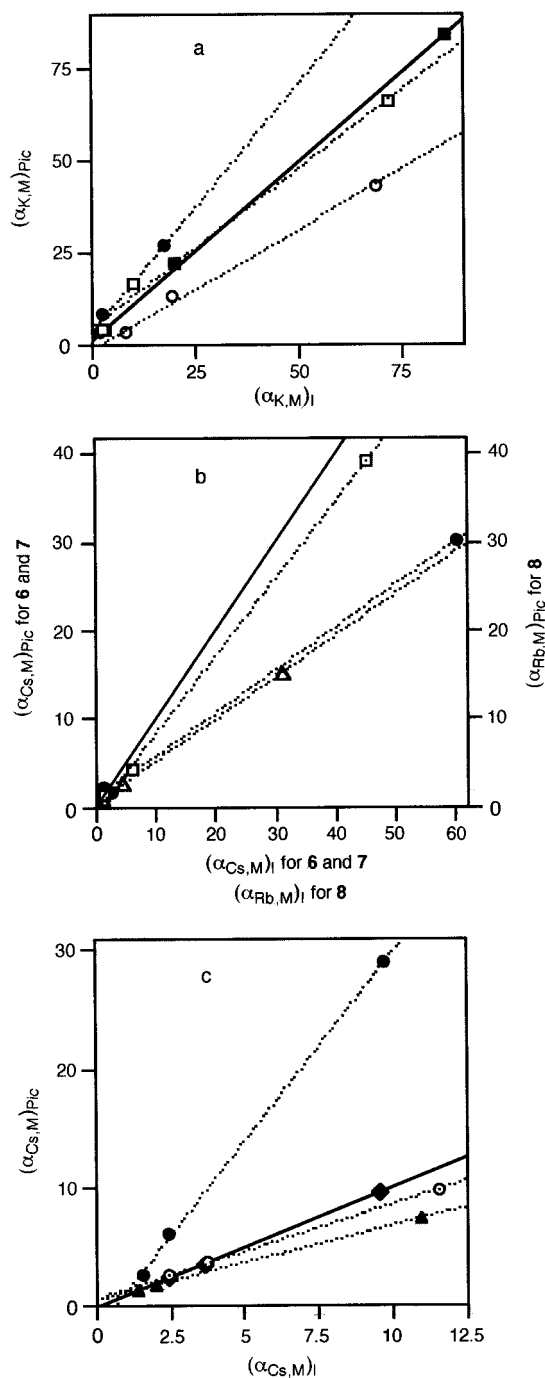


**Figure 2.** Correlation of separation factors  $(\alpha_{M_1,M_2})_{Pic}$  and  $(\alpha_{M_1,M_2})_I$  for competitive alkali metal ion extractions from aqueous picrate and iodide solutions with  $CHCl_3$  solutions of (a) 18-crown-6 derivatives **1** ( $\square$ , slope 0.83), **2** ( $\bullet$ , slope 1.46), **4** ( $\circ$ , slope 0.58), and **5** ( $\blacksquare$ , slope 0.96) ( $M_1 = K$  and  $M_2 = Na, Rb,$  and  $Cs$ ), (b) 21-crown-7 derivatives **6** ( $\square$ , slope 0.88) and **7** ( $\Delta$ , slope 0.47) ( $M_1 = Cs$  and  $M_2 = Na, K,$  and  $Rb$ ), and **8** ( $\bullet$ , slope 0.48) ( $M_1 = Rb$  and  $M_2 = Na, K,$  and  $Cs$ ), and (c) 24-crown-8 derivatives **9** ( $\circ$ , slope 0.80), **10** ( $\blacklozenge$ , slope 1.02), **11** ( $\bullet$ , slope 3.18), and **13** ( $\blacktriangle$ , slope 0.62) ( $M_1 = Cs$  and  $M_2 = Na, K,$  and  $Rb$ ). (Solid lines with slope of 1 are included for comparison. None of the graphs showed a correlation coefficient  $r^2$  below 0.98).

21-crown-7 compound was noted to produce a change from slight  $Cs^+/Rb^+$  extraction selectivities for benzo-21-crown-7 (B21C7, **6**) and dibenzo-21-crown-7 (DB21C7, **7**) to moderate  $Rb^+/Cs^+$  selectivity for tribenzo-21-crown-7 (TB21C7, **8**). Therefore,  $\alpha_{Cs,M}$  values were used for characterization of the alkali metal ion selectivities of **6** and **7**, while for extractions by **8**,  $\alpha_{Rb,M}$  values were calculated.

The correlations between the corresponding separation factors  $(\alpha_{M_1,M_2})_{Pic}$  vs  $(\alpha_{M_1,M_2})_I$  for 21-crown-7 compounds are presented in Figure 2b. The lines for **6**, **7**, and **8** have slopes of 0.88, 0.47, and 0.48, respectively. Therefore, the extraction selectivities of these benzo group-containing CEs decrease when the aqueous phase anion is changed from  $I^-$  to  $Pic^-$ . Based on the slope value that may be considered as a measure of an average magnitude of deviation of the  $(\alpha_{M_1,M_2})_{Pic}$  from that of the  $(\alpha_{M_1,M_2})_I$ , the “picrate effect” for **6** which has only one aromatic moiety may be viewed as insignificant. However, for **7** and **8** which contain two and three benzo groups, respectively, an average 2-fold decrease in selectivity is observed when  $Pic^-$  was the counterion.

(c) **Extractions by 24-Membered CEs.** To probe the “picrate effect” on the alkali metal cation extraction selectivities of 24-membered CEs, compounds **9–13** with differing numbers and locations of benzo groups were employed. Ligands **11** and **13** (TB24C8-1 and TB24C8-2, respectively) are positional isomers of tribenzo-24-crown-8.

Correlations of the separation factors  $(\alpha_{Cs,M})_{Pic}$  vs  $(\alpha_{Cs,M})_I$  for the competitive alkali metal cation extractions by **9–11** and **13** are shown in Figure 2c. For benzo-24-crown-8 (B24C8, **9**) and dibenzo-24-crown-8 (DB24C8, **10**), no significant deviation of the extraction selectivities with the anion variation are evident. However, when the number of benzo groups in the CE was increased to three in **11** and **13**, the “picrate effect” on the separation ability of the ligands for alkali metal cations becomes obvious. Moreover, consistent with the opposite effects of the anion variation on the selectivities of DB18C6 and *unsym*-DB18C6, the two isomers of TB24C8, **11** and **13**, exhibit opposite changes in  $Cs^+/M^+$  selectivities on going from  $I^-$  to  $Pic^-$  as the anion. Specifically, the  $\alpha_{Cs,M}$  values for **11** increased by a factor of 3 when  $I^-$  was replaced with  $Pic^-$  (the slope for the plot  $(\alpha_{Cs,M})_{Pic}$  vs  $(\alpha_{Cs,M})_I$  was 3.18 for this CE), whereas for **13**, an average decrease of  $Cs^+$  selectivity by half was observed for the same anion variation (the slope is 0.62). This provides another example of the dependence of the “picrate effect” on the location of the aromatic groups in the macrocycle.

For both competitive alkali metal picrate and iodide extractions by tetrabenzo-24-crown-8 (TetB24C8, **12**), precipitation was observed in the organic phase. The yellow solid obtained from the extraction with  $Pic^-$  in the aqueous solution was found to contain only  $Cs^+$  and  $Rb^+$  ions in an approximate ratio of 3.5:1.<sup>13</sup> In contrast, the precipitate resulting from the alkali metal iodide extraction with **12** contained predominantly  $Cs^+$  ions, with traces of  $Na^+$ . No  $Rb^+$ ,  $K^+$ , or  $Li^+$  ions were detected in this solid. Hence, the use of  $Pic^-$  instead of  $I^-$  as the aqueous phase anion significantly decreased the selectivity of  $Cs^+$  separation from the mixture of alkali metal cations by TetB24C8.

Thus, the “picrate effect” on extraction selectivities of a variety of benzo group-containing CEs for alkali metal cations has been appraised. To provide insight into the  $\pi$ - $\pi$  interactions between  $Pic^-$  and benzo groups of the CEs as the potential causative factor for the observed extraction behaviors of the ionophores, structural studies for the alkali metal picrate complexes of the CEs in the solid state and in solution were undertaken.

**Crystal Structures of the Alkali Metal Picrate Complexes with Benzo Group-Containing CEs.** We have determined crystal structures of nine complexes: KPic-2, RbPic-2, KPic-3, KPic-4, RbPic-4, RbPic-8, CsPic-11, RbPic-12, and CsPic-12. This series includes structures of alkali metal picrate complexes with DB18C6, *unsym*-DB18C6, TB18C6, TB21C7, TB24C8-1, and TetB24C8. Picrate-CE benzo group interactions

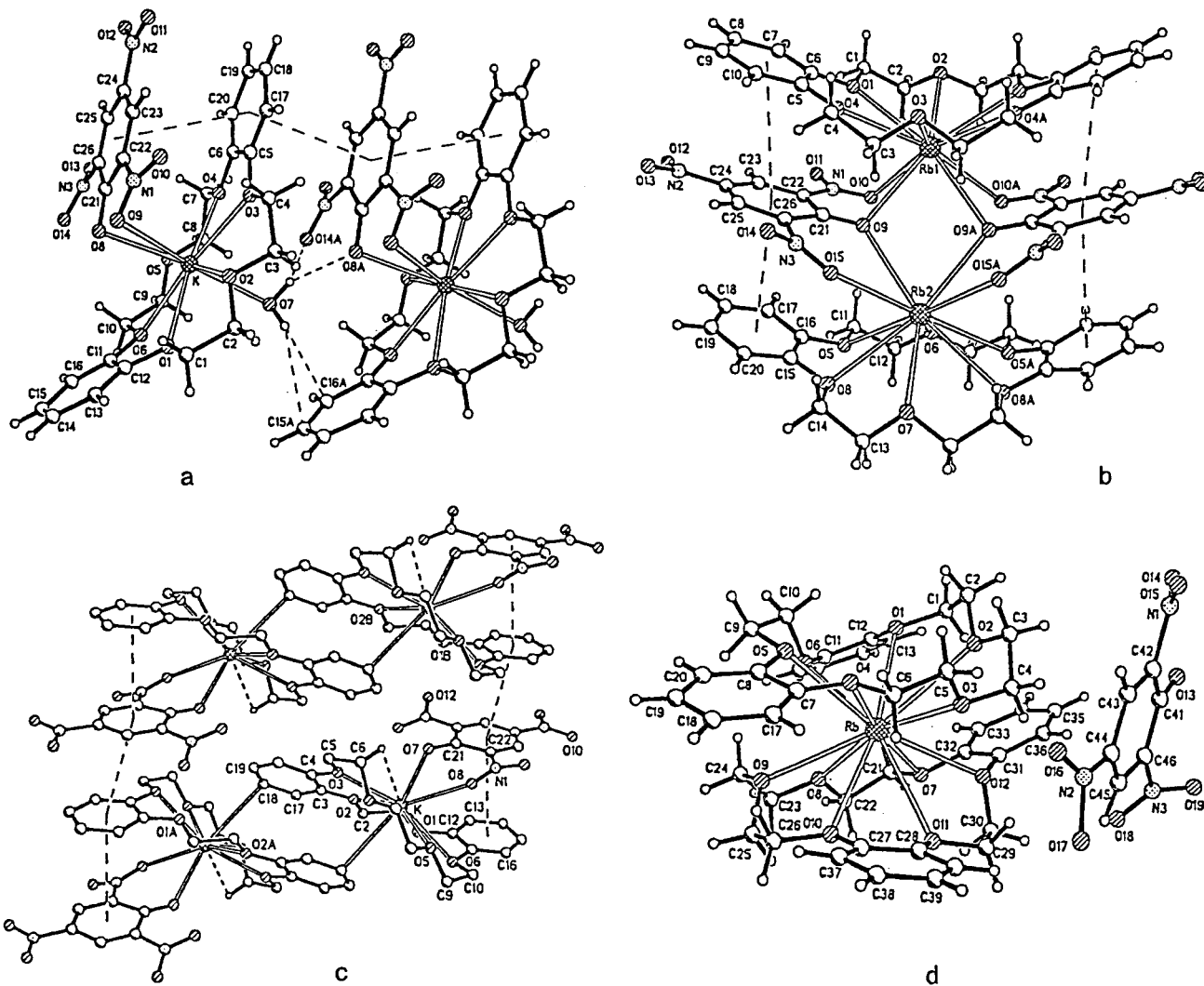


**Figure 3.** Crystal structures of the alkali metal picrate complexes with the isomeric dibenzo-18-crown-6 ligands (a) KPic-4, (b) RbPic-4, (c) KPic-2, and (d) RbPic-2.

were found in eight of the nine complexes. A detailed discussion of the structures is provided in the Supporting Information. The discussion which follows focuses only on the stacking of Pic<sup>-</sup> with aromatic groups of the CEs.

**(a) Crystal Structures of the DB18C6 Complexes, KPic-4 and RbPic-4.** In the structure of complex KPic-4 (Figure 3a), where K<sup>+</sup> is coordinated to all six ether oxygen atoms of the CE, two oxygens of Pic<sup>-</sup>, and an oxygen atom of the water molecule, face-to-face aromatic stacking of Pic<sup>-</sup> and one benzo substituent of DB18C6 is observed. The neutral complexes comprise the asymmetric unit column along the unit cell direction *a* to form stacks of alternating Pic<sup>-</sup> moieties and the C5, C6, C17–C20 benzo rings of the CE. The strength of this  $\pi$ - $\pi$  interaction may be estimated from the centroid–centroid distances for these aromatic groups. The two unique separations of the coplanar Pic<sup>-</sup> and benzo moieties (within the same asymmetric unit and between the asymmetric units related by a unit translation along *a*) are 4.026 and 3.882 Å, respectively.

Since the larger Rb<sup>+</sup> cannot reside as deeply in the DB18C6 cavity as K<sup>+</sup>, it perches above the mean plane of the CE. The complex RbPic-4 has a dimeric structure (Figure 3b). The Rb<sup>+</sup> ions in the dimeric complex coordinate opposite faces of the two CE moieties which facilitates their face-to-face stacking with the Pic<sup>-</sup> anions. The centroid–centroid separations between Pic<sup>-</sup> and the C15–C20 benzo ring and another Pic<sup>-</sup> and the C5–C10 benzo group are 3.674 and 3.863 Å, respectively.

These distances are shorter than the centroid–centroid separations observed for the stacked anion and CE benzo group in the KPic-4 complex. This indicates that the Pic<sup>-</sup>–ligand interactions in the Rb<sup>+</sup> complex of DB18C6 are stronger than those in the K<sup>+</sup> complex of this CE.

**(b) Crystal Structures of the unsym-DB18C6 Complexes, KPic-2 and RbPic-2.** Similar to the structure of KPic-4, K<sup>+</sup> in KPic-2 resides deeply in the CE cavity and coordinates with all of the macrocyclic oxygens and two oxygen atoms of the Pic<sup>-</sup> (Figure 3c). However, in contrast with KPic-4, the coordination sphere of K<sup>+</sup> on the opposite side of the CE is now completed by dimerization of the complex via interaction of the metal ion with a benzo ring of the neighboring CE unit. The coordinated Pic<sup>-</sup> and another benzo group of **2** are involved in face-to-face stacking forming alternating Pic<sup>-</sup>/benzo ring columns along the unit cell direction *a*. The centroid–centroid distances within the asymmetric unit and between the asymmetric units are 3.745 and 3.895 Å, respectively. Therefore, the stacking of Pic<sup>-</sup> and a benzo moiety in the KPic complex of unsym-DB18C6 is stronger than that in the analogous complex of the symmetrical isomer of DB18C6.

In contrast, the crystal structure of complex RbPic-2 is the only one of the nine that does not exhibit any picrate–CE benzo group stacking interactions. Instead, RbPic-3 crystallizes as a 2:1 (CE-to-metal) sandwich complex (Figure 3d).

**(c) Crystal Structure of the TB18C6 Complex, KPic-3.**

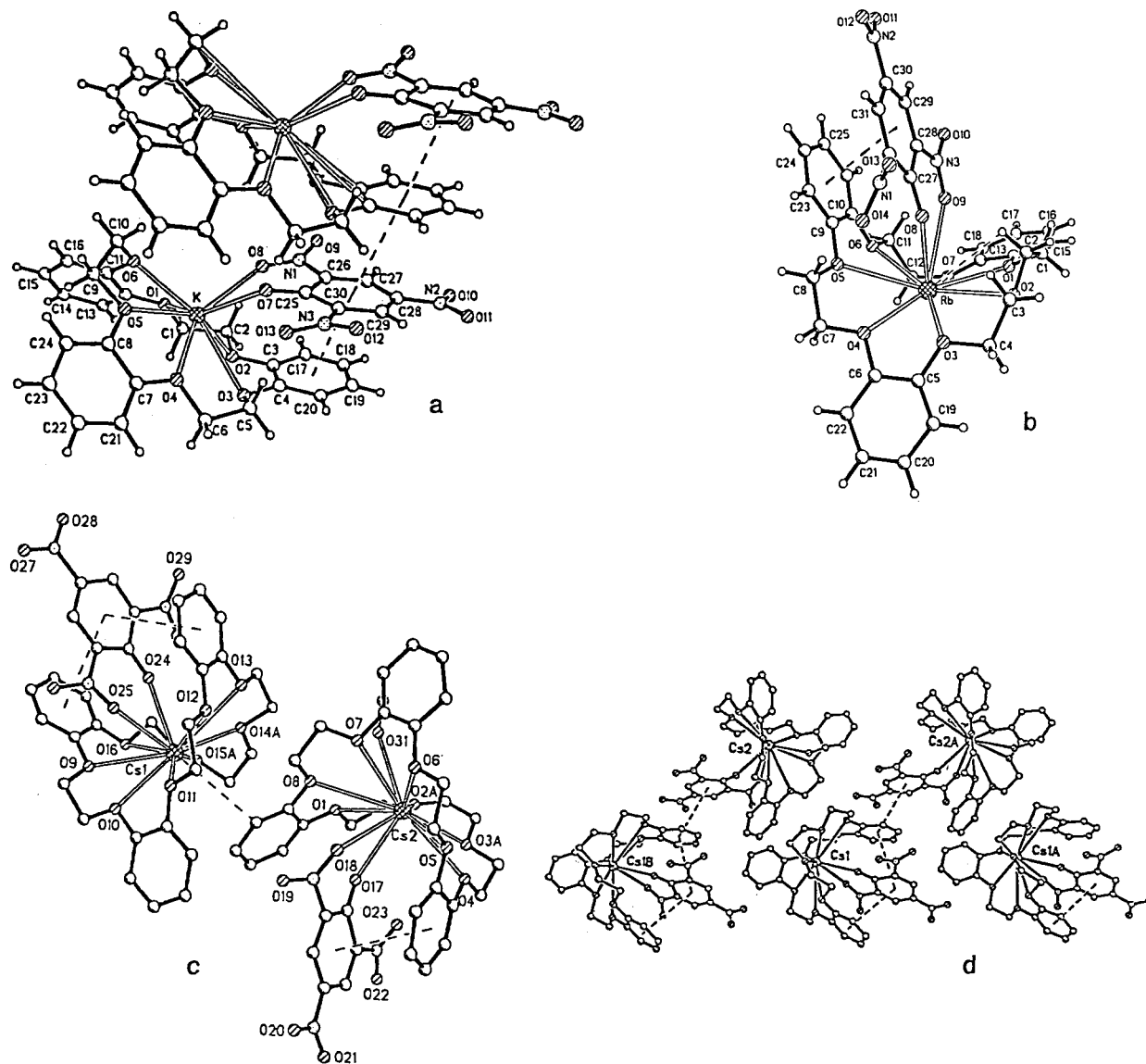


**Figure 4.** Crystal structures of the alkali metal picrate complexes with the 18-, 21-, and 24-membered tribenzo-CEs (a) KPic-3, (b) RbPic-8, and (c and d) CsPic-11.

Since the more rigid TB18C6 cannot coordinate  $K^+$  within the mean plane formed by its oxygens, the metal ion resides appreciably above the CE cavity (Figure 4a). This allows  $Pic^-$  to have closer face-to-face stacking with the CE benzo group. Thus, the anion and the C3, C4, C17–C20 benzo ring exhibits a centroid–centroid separation of 3.720 Å in the asymmetric unit and of only 3.613 Å between the asymmetric units. This interaction produces stacked columns along the *a* axis with a length (7.2884(5) Å) that compares favorably with those values found for KPic-2 and KPic-4, which have similar anion–CE stacking features.

**(d) Crystal Structure of the TB21C7 Complex, RbPic-8.** The larger 21-membered macrocycle **8** allows  $Rb^+$  to penetrate deeply into the CE cavity (Figure 4b). The coordinated  $Pic^-$  is arranged so that it forms face-to-face stacking with the C9, C10, C23–C26 benzo ring of TB21C7 with a centroid–centroid separation of 3.817 Å.

**(e) Crystal Structure of the TB24C8 Complex, CsPic-11.** This structure illustrates the variability of a larger, more flexible CE in satisfying both the metal ion coordination arrangement and any  $Pic^-$ –CE benzo ring stacking interactions. In the structure of CsPic-11, there are two unique  $Cs^+$ -complex

species as shown in Figure 4c. In one of them, the  $Pic^-$  coordinated to Cs1 forms face-to-face stacking with two of the benzo rings of TB24C8 with the centroid–centroid separations of 4.195 and 4.036 Å. These two CE benzo rings are also face-to-face stacked with the other unique CsPic–TB24C8 complex species (Figure 4d).

**(f) Crystal Structures of the TetB24C8 Complexes, RbPic-12 and CsPic-12.** The structure of the complex CsPic-12 is presented in Figure 5. The complex RbPic-12 is isostructural with its  $Cs^+$ -containing analogue. In both of the complexes, opposing benzo substituents of **12** fold over one another to form two large clefts which make the metal ion accessible for further coordination with the anion.  $Pic^-$  plays a remarkable role in the structures of RbPic-12 and CsPic-12. Its coordination with the metal cations may be assisted by face-to-face stacking with the CE benzo substituents that form the cleft. The  $Pic^-$  units bridge the two metal centers in a head-to-tail manner forming infinite coordination polymers. As a result, each  $Pic^-$  is “sandwiched” between four benzo groups from the CEs.

**$^1H$  NMR Spectra of the Alkali Metal Picrate Complexes with Benzo Group-Containing CEs.** Although  $\pi$ -stacking of

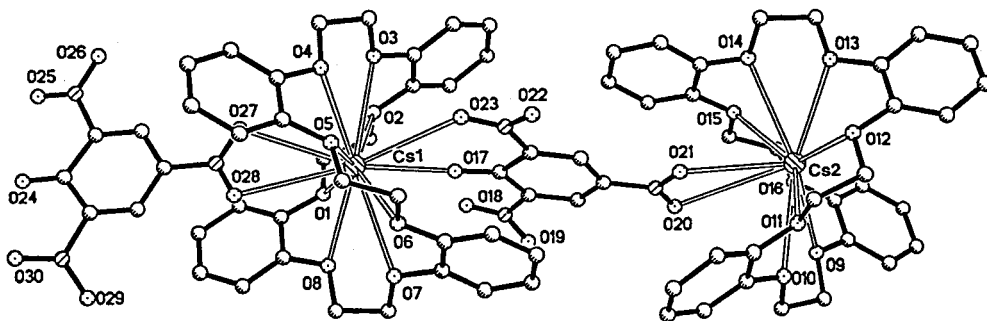


Figure 5. Crystal structure of the CsPic complex with tetrabenzo-24-crown-8 (CsPic-12).

Pic<sup>-</sup> with the benzo groups of the CE was evident in most of the crystal structures for the MPic-CE complexes, the complex geometry in solution, where complexation/decomplexation equilibria, conformational dynamics, and various interactions involving solvent molecules take place, may vary from that in the solid state. To provide insight into  $\pi$ - $\pi$  interactions between Pic<sup>-</sup> and benzo-substituted CEs 1-13 in CHCl<sub>3</sub> (the solvent used as the organic phase in the extraction), <sup>1</sup>H NMR spectroscopy was employed for the investigation of MPic-CE complexes (excluding LiPic) in CDCl<sub>3</sub> solution.

The spectra of the CEs showed significant, sophisticated changes on complexation with alkali metal cations<sup>15</sup> due to electronic and conformational effects (which will not be discussed in this paper). This made the signals for the CE protons unsuitable for investigation of the anion-ligand interactions. In contrast, the singlet of Pic<sup>-</sup> protons appeared to be very convenient to probe for possible  $\pi$ - $\pi$  interactions between Pic<sup>-</sup> and benzo groups of the CE.

Changes in the chemical shift for Pic<sup>-</sup> protons on complexation of metal picrates with aromatic group-containing macrocycles have been observed earlier (for example, see ref 9c). However, these changes and their variation with altered identity of the metal cation and/or macrocyclic ligand have not been used for systematic investigation of the Pic<sup>-</sup>-ionophore  $\pi$ -stacking, to the best of our knowledge.

The CE-alkali metal picrate complexes were prepared by dissolution of the solid MPic salt in a CDCl<sub>3</sub> solution of the CE. Since the solubility of the alkali metal picrates themselves in chloroform is negligibly small, they are transferred into the organic solution only through complexation with the CE. Therefore, it was impossible to compare the NMR spectra of uncomplexed MPic with those of the MPic-CE complexes in CDCl<sub>3</sub>. Hence, the spectral characteristics of the MPic complexes with the benzo-substituted CEs were compared with those for complexes of related CEs that contain no aromatic units. The chemical shifts,  $\delta_{\text{H-Pic}}$ , determined for the alkali metal picrate complexes of the 18-crown-6-type ligands and also of the 21- and 24-membered CEs are presented in Figure 6 and Table 1, respectively.

In the spectra for all of the MPic complexes with the benzo derivatives of 18-crown-6, the singlets for the Pic<sup>-</sup> protons were observed upfield from those of the complexes with DC18C6 (5) (Figure 6a). Similarly, the  $\delta_{\text{H-Pic}}$  of the alkali metal picrate complexes with benzo group-containing 21- and 24-membered CEs were smaller than those for the complexes of dicyclohexano-21-crown-7 (DC21C7, 14) and 24-crown-8 (24C8, 15),<sup>16</sup>

(15) This problem has been discussed in numerous publications, beginning with the following: Live, D.; Chan, S. I. *J. Am. Chem. Soc.* **1976**, *98*, 3769-3778.

(16) Since commercially available dicyclohexano-24-crown-8 contains some quantity of dibenzo-24-crown-8 which may be critical for the results of this study, we utilized 24-crown-8 (15) instead.

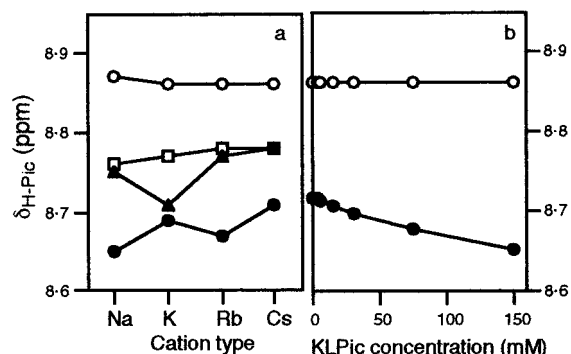


Figure 6. Chemical shifts of Pic<sup>-</sup> protons,  $\delta_{\text{H-Pic}}$ , in the <sup>1</sup>H NMR spectra (CDCl<sub>3</sub>) of alkali metal picrate complexes of 1 (□), 2 (▲), 4 (●), and 5 (○) vs (a) the alkali metal cation and (b) concentration of the K<sup>+</sup>LPic<sup>-</sup> complex.

Table 1. Chemical Shift Values for Picrate Protons in the <sup>1</sup>H NMR Spectra of Alkali Metal Picrate Complexes of 21- and 24-Membered CEs in CDCl<sub>3</sub> (200 MHz, 297K)<sup>a</sup>

macrocyclic type	CE <sup>b</sup>	$\delta_{\text{H-Pic}}$ (ppm) for the MPic complex where M is			
		Na	K	Rb	Cs
21-crown-7	14	8.86	8.85	8.84	8.84
	6	8.81	8.73	8.73	8.73
	7	8.72	8.67	8.68	8.69
	8	8.65	8.59	8.64	8.66
24-crown-8	15	8.87	8.86	8.84	8.84
	9	8.80	8.77	8.75	8.75
	10	8.77	8.69	8.69	8.73
	11	8.73	8.62	8.61	8.62
	13	8.69	8.63	8.65	8.65
	12	8.61	8.60	8.53	8.54

<sup>a</sup> Solutions of the complexes were prepared by dissolving solid metal picrates in 30.0 mM solutions of the CEs in CDCl<sub>3</sub>. <sup>b</sup> The CEs are listed in the order of the increasing number of benzo groups.

respectively. Such increased shielding of the Pic<sup>-</sup> protons is believed to result from Pic-CE  $\pi$ - $\pi$  interactions.

The  $\delta_{\text{H-Pic}}$  values for MPic complexes of the benzo-substituted ligands may change significantly when the cation is varied (Figure 6a and Table 1). In contrast, when no aromatic substituent is present in the CE (5, 14, and 15), only a very slight tendency for smaller  $\delta_{\text{H-Pic}}$  values on going from Na<sup>+</sup> to Cs<sup>+</sup> was observed. This tendency was unaffected by variation of the macrocycle size and, therefore, cannot be explained by differing stabilities of the complex cations M<sup>+</sup>L or the type of ion pairs M<sup>+</sup>LPic<sup>-</sup> for these CEs.<sup>17</sup> In addition, as shown in Figure 6b for KPic complexes of DB18C6 (4) and DC18C6

(17) Only very small changes of the  $\delta_{\text{H-Pic}}$  value were observed with cation identity variation for the alkali metal picrate complexes of the CEs containing no aromatic moieties. The  $\delta_{\text{H-Pic}}$  value exhibited a consistent, very small decrease in the order Na<sup>+</sup> > K<sup>+</sup> ≥ Rb<sup>+</sup> = Cs<sup>+</sup> which may be caused by different solvation of the cations by water present in CDCl<sub>3</sub> that was used without prior drying.

(5), shielding of the Pic<sup>-</sup> protons in the spectrum of K<sup>+</sup>(4)Pic<sup>-</sup> varied when the complex concentration in solution was changed, while  $\delta_{\text{H-Pic}}$  for K<sup>+</sup>(5)Pic<sup>-</sup> was essentially insensitive to concentration variations.<sup>18</sup> This suggests that the value of  $\delta_{\text{H-Pic}}$  for the alkali metal picrate complexes formed by CEs which contain one or more benzo units reflects an equilibrium between the complex species in which different modes of the anion-CE stacking are present and also those species in which such stacking is absent. Hence, a larger upfield shift of the Pic<sup>-</sup> proton signals in the spectrum of the MPic-CE indicates a greater population of species with  $\pi$ - $\pi$  interactions.

From the data in Figure 6a and Table 1, it is evident that shielding of the Pic<sup>-</sup> protons in the complexes with benzo-substituted CEs increases as the number of benzo groups in the macrocycle is enhanced. The only exception to this trend was noted in the  $\delta_{\text{H-Pic}}$  values for the MPic complexes of TB18C6 (3, not shown in Figure 6a), which were 8.70, 8.73, 8.73, and 8.72 ppm for Na<sup>+</sup>(3)Pic<sup>-</sup>, K<sup>+</sup>(3)Pic<sup>-</sup>, Rb<sup>+</sup>(3)Pic<sup>-</sup>, and Cs<sup>+</sup>(3)Pic<sup>-</sup>, respectively. The unexpectedly higher  $\delta_{\text{H-Pic}}$  values for these complexes may be caused by their relatively low concentrations in solution.<sup>19</sup>

If  $\pi$ - $\pi$  interaction between the Pic<sup>-</sup> and an aromatic substituent of the CE takes place, it is expected also to affect the spectrum of the ligand in the region of the aromatic proton signals. As illustrated in Figure 7 for 1, chemical shifts and shapes of the signals for the benzo group protons of the CEs change significantly in going from the uncomplexed ligands to their alkali metal picrate complexes. These changes are caused by both CE-Pic<sup>-</sup> and CE-cation interactions, which is evident from a comparison of the spectrum for 4 (Figure 7a) with those of K<sup>+</sup>(4)Pic<sup>-</sup> (in which both cation and anion may interact with the ligand) and of K<sup>+</sup>(4)I<sup>-</sup> (in which only CE-cation interaction is anticipated) (Figures 7c and 7b, respectively).

Estimation of the contribution from the ligand-Pic<sup>-</sup> interaction to the changes observed for the spectrum of K<sup>+</sup>(4)Pic<sup>-</sup> relative to that of the uncomplexed DB18C6 would require more extensive investigation which is outside the scope of the present work. Nevertheless, the upfield shift observed for signals of the DB18C6 aromatic protons in the KPic complex compared to the KI complex provides additional support for the proposed  $\pi$ -stacking of Pic<sup>-</sup> with a benzo group of the CE.

Although a smaller  $\delta_{\text{H-Pic}}$  value for an alkali metal picrate complex with the CE-containing benzo groups is associated with a larger population of the complex species involving Pic<sup>-</sup>-CE interactions, characterization of the Pic<sup>-</sup>-CE adduct stability based on the  $\delta_{\text{H-Pic}}$  value is complicated. It should take into account that shielding of the Pic<sup>-</sup> protons due to the anion-CE stacking depends significantly on the geometry of the complex. In particular, its magnitude will be greater for complexes in which Pic<sup>-</sup> is involved in stacking with several benzo groups of the CE than those in which the anion interacts with only one aromatic substituent of the ionophore. Also, in addition to face-to-face Pic<sup>-</sup>-aromatic moiety  $\pi$ - $\pi$  stacking, a face-to-edge mode is possible. These two dissimilar anion-CE interactions may induce opposing changes in the chemical shifts of the Pic<sup>-</sup> protons. Last, although the thermodynamic

(18) Analogously, the  $\delta_{\text{H-Pic}}$  values for the MPic complexes of DC21C7 (14) and 24C8 (15) in CDCl<sub>3</sub> were insensitive to changes in the concentration of the complex, in contrast with those for the MPic complexes of the benzo group-containing 21- and 24-membered CEs.

(19) Due to the significantly weaker complexing ability of rigid TB18C6 for NaPic, RbPic, and CsPic relative to those of the mono- and dibenzo-18C6 compounds, the solubilities of these solid alkali metal picrates in CDCl<sub>3</sub> in the presence of 3 were considerably lower than that for 1, 2, and 4. Although 3 exhibited appreciable binding ability for KPic, the complex KPic-3 had limited solubility in CHCl<sub>3</sub>.

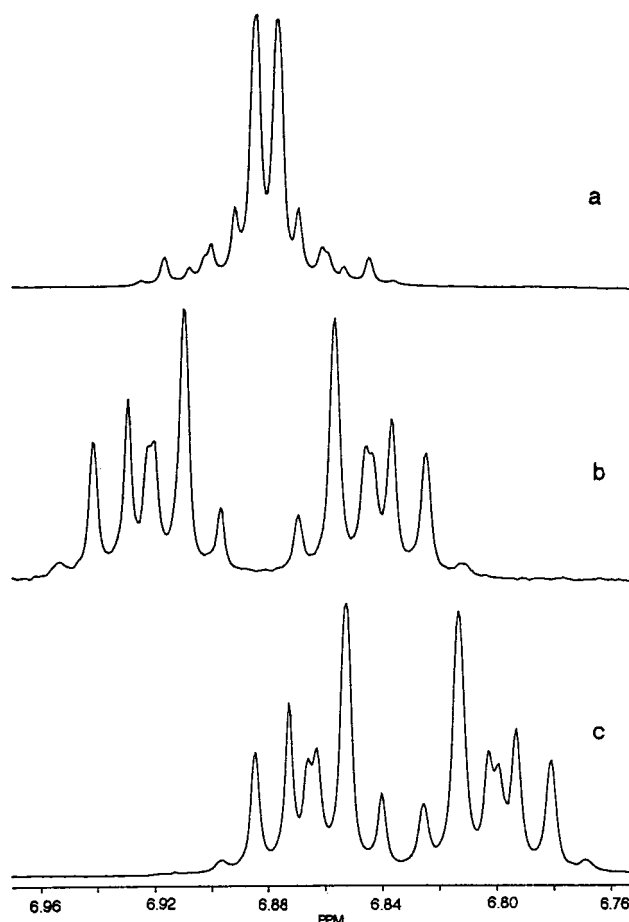


**Figure 7.** Aromatic region of the <sup>1</sup>H NMR spectra (30.0 mM in CDCl<sub>3</sub>, 300 MHz, 297K) of (a) 4 and its complexes with (b) KI and (c) KPic.

stability of the complex M<sup>+</sup>LPic<sup>-</sup>, unlike its geometry, is not a principal factor for the Pic<sup>-</sup>-CE  $\pi$ -stacking formation, it will determine the concentration of the complex species in solution and, therefore, may have some effect on the observed  $\delta_{\text{H-Pic}}$  value.

Thus, the increasing shielding of the Pic<sup>-</sup> protons indicates enhanced anion-ligand  $\pi$ - $\pi$  interaction in the alkali metal picrate complexes; but the  $\delta_{\text{H-Pic}}$  value may not be taken to be a measure of the contribution from Pic<sup>-</sup>-CE  $\pi$ -stacking to the overall complex stability. Therefore,  $\delta_{\text{H-Pic}}$  for the MPic-CE complexes cannot be related directly to the change of the CE extraction selectivity for alkali metal ions observed when the aqueous phase anion is varied from I<sup>-</sup> to Pic<sup>-</sup>. Nevertheless, some interesting correlations of the CE extraction behavior with the spectral characteristics of the alkali metal picrate complexes in solution and also their structural features in the solid state have emerged.

**Correlations between the "Picrate Effect" on CE Extraction Selectivities and CE-Pic<sup>-</sup>  $\pi$ -Stacking Observed for the CE-Alkali Metal Picrate Complexes in Solution and in the Solid State.** The best expressed correlation is noted for the series of benzo group-substituted 18-membered CEs, B18C6 (1), DB18C6 (4), and *unsym*-DB18C6 (2). Thus, ligand 1, which contains only a single aromatic moiety, exhibits only very small deviation of the extraction selectivity for alkali metal picrates from that for iodides (Figure 2a). In agreement, the  $\delta_{\text{H-Pic}}$  values observed in the NMR spectra of the MPic-1 complexes, which were further downfield than those for the complexes of dibenzo and tribenzo derivatives of 18-crown-6, are also relatively insensitive to changes of the alkali metal cation (Figure 6a).



In the NMR spectra for the series of MPic complexes of the unsymmetrical dibenzo-substituted **2**, the largest upfield shift of the Pic<sup>-</sup> proton signals due to the  $\pi$ - $\pi$  interactions is observed for the K<sup>+</sup> complex (Figure 6a). Therefore, the solution of K<sup>+</sup>(**2**)Pic<sup>-</sup> must have the greatest population of species in which the  $\pi$ -stacking is involved. Consistent with the NMR data in solution, face-to-face  $\pi$ - $\pi$  stacking of Pic<sup>-</sup> with a benzo group of *unsym*-DB18C6 is clearly evident in the solid-state structure of the KPic-**2** complex (Figure 3c), but is absent in the analogous complex with RbPic (Figure 3d). These structural features of the complexes are in agreement with the observed enhancement of the K<sup>+</sup> selectivity of *unsym*-DB18C6 in the extraction of alkali metal picrates relative to that of the iodides (Figure 2a).

In the NMR spectra of all four of the alkali metal picrate complexes of symmetrical DB18C6 (**4**), the  $\delta_{\text{H-Pic}}$  values are smaller than those for the other benzo group-containing 18-membered CEs **1**-**3** (Figure 6a), which indicates that in the solutions of these complexes, the proportion of species with Pic<sup>-</sup>-**4** interactions is relatively large. The solid-state structural data support the solution behavior of the MPic-**4** complexes. Thus, face-to-face  $\pi$ - $\pi$  stacking of Pic<sup>-</sup> with benzo groups of the CE is observed in the crystal structures of both KPic-**4** (Figure 3a) and RbPic-**4** (Figure 3b). However, the magnitude of the Pic<sup>-</sup>-CE benzo ring separations assessed from the solid-state structures of these complexes indicates that the anion-ligand interaction in KPic-**4** is weaker than that in the dimeric RbPic-**4**. In agreement, the shielding of the Pic<sup>-</sup> protons in the NMR spectrum of the Rb<sup>+</sup> complex of **4** is greater than that for the K<sup>+</sup> complex of this CE (Figure 6a). Similarly, the  $\delta_{\text{H-Pic}}$  value for Na<sup>+</sup>(**4**)Pic<sup>-</sup> is smaller than that for K<sup>+</sup>(**4**)Pic<sup>-</sup>. Therefore, on the basis of the solution NMR data and the solid-state structures of the MPic-DB18C6 complexes, anion-CE interactions are believed to be more significant in NaPic-**4** and RbPic-**4** than in the analogous complex with KPic (in contrast with the ordering of increasing thermodynamic stability of the complexes). In agreement, the extraction selectivity of **4** for K<sup>+</sup> over other alkali metal cations decreases when the aqueous phase anion is changed from I<sup>-</sup> to Pic<sup>-</sup> (Figure 2a).

The Pic<sup>-</sup>-CE  $\pi$ - $\pi$  stacking which evidently enhances the stability of the KPic-**3** crystal lattice (Figure 4a) is believed to be responsible for the selective precipitation of this complex from the organic phase after the competitive extraction of alkali metal picrates with TB18C6 and, thus, for dramatic change of the separation ability for **3** from slight preference of Rb<sup>+</sup> and Cs<sup>+</sup> over K<sup>+</sup> with I<sup>-</sup> as the anion to appreciable K<sup>+</sup>/Rb<sup>+</sup> and K<sup>+</sup>/Cs<sup>+</sup> selectivity with Pic<sup>-</sup>.

Some interesting observations may be made also for the series of benzo-substituted 21-crown-7 derivatives. Thus, for DB21C7 (**7**) and especially TB21C7 (**8**), which are known for preferential binding of the larger alkali metal cations (Cs<sup>+</sup> and Rb<sup>+</sup>, respectively), the greatest upfield shifts of the Pic<sup>-</sup> proton signals in the NMR spectra were observed unexpectedly for their K<sup>+</sup> complexes (Table 1). (This is another example of the  $\pi$ -stacking being controlled by structural factors rather than complex stability.) In agreement, the Cs<sup>+</sup>/M<sup>+</sup> extraction selectivity of **7** and Rb<sup>+</sup>/M<sup>+</sup> selectivity of **8** decreased on the average by half when Pic<sup>-</sup> was used as a counterion instead of I<sup>-</sup> (Figure 2b). Specifically, the separation factors ( $\alpha_{\text{Rb,K}}^{\text{Pic}}$ ) and ( $\alpha_{\text{Rb,K}}^{\text{I}}$ ) of **8** were 1.46 and 3.58, respectively.

For the largest sized 24-crown-4 derivatives, the effect of Pic<sup>-</sup> on the extraction selectivities for alkali metal ions does not correlate as clearly with the NMR spectral characteristics of the MPic-CE complexes as do those for the 18- and 21-

membered ligands. Nevertheless, certain correlations are worth mentioning. In particular, the two positional isomers of TB24C8, **11** and **13**, whose selectivity  $\alpha_{\text{Cs,M}}$  in the competitive alkali metal ion extractions responded oppositely<sup>20</sup> to variation of the aqueous phase anion (Figure 2c), also exhibit distinctive changes of the  $\delta_{\text{H-Pic}}$  values in the NMR spectra when the identity of alkali metal cation in the complex M<sup>+</sup>LPic<sup>-</sup> is varied (Table 1). For **11**, whose extraction selectivity for Cs<sup>+</sup> over other alkali metal cations increased on the average 3-fold with Pic<sup>-</sup> as the counterion, numerous Pic<sup>-</sup>-CE stackings are clearly evident in the solid-state structure of the CsPic-**11** complex (Figures 4c and 4d).

The ability of TetB24C8 (**12**) to differentiate between Cs<sup>+</sup> and Rb<sup>+</sup> during competitive alkali metal picrate extraction was significantly decreased relative to that for the iodides due to coprecipitation of two complexes, CsPic-**12** and RbPic-**12**, from the organic phase. In the solid-state structures of these isostructural compounds (Figure 5), multiple TetB24C8-Pic<sup>-</sup> interactions are present. In agreement, the NMR spectra of Cs<sup>+</sup>(**12**)Pic<sup>-</sup> and Rb<sup>+</sup>(**12**)Pic<sup>-</sup> in CDCl<sub>3</sub> (Table 1) showed comparable, upfield shifts of the largest magnitude for the Pic<sup>-</sup> proton signals among those for the alkali metal picrate complexes of benzo group-containing CEs, despite the limited solubility of CsPic-**12** and RbPic-**12** in chloroform and, therefore, relatively small concentrations of these complexes in solution.

Thus, the "picrate effect" has been evaluated for the wide variety of benzo group-containing CEs. We envision that similar influences of Pic<sup>-</sup> on the separation abilities of other types of aromatic group-containing macrocyclic ligands, e.g., lariat ethers, calixarenes, or cryptands, may be found. However, it should be noted that the importance of the Pic<sup>-</sup>-CE  $\pi$ - $\pi$  interactions may be altered by the presence of bulky or electron-withdrawing substituents in the benzo moieties or in the macrocycle itself due to steric or electronic factors, respectively.

## Conclusions

The use of Pic<sup>-</sup> as the aqueous phase anion for solvent extraction of alkali metal cations with benzo group-containing CEs may significantly influence the magnitude of the selectivity in metal ion separation (and sometimes the selectivity order) relative to that for the extraction of alkali metal salts with inorganic anions. The importance of the "picrate effect" is found to increase with the number of benzo substituents in the CE and vary with their positioning in the macrocycle. Based on the structural data obtained in solution and the solid state, the "picrate effect" on extraction selectivities of the benzo group-containing CEs is believed to result from  $\pi$ - $\pi$  interactions between Pic<sup>-</sup> and one or more aromatic units in the ionophore. This study clearly demonstrates that anion-ligand interactions within the macrocyclic complex, which often are neglected, may play an important role in metal salt complexation by crown ether compounds.

## Experimental Section

**Instrumentation.** Concentrations of alkali metal ions in aqueous solution were determined by ion chromatography with a Dionex DX-120 ion chromatograph. <sup>1</sup>H NMR spectra were recorded with IBM AF-200 (200 MHz) and IBM AF-300 (300 MHz) spectrometers with use of TMS as the internal standard.

(20) Interestingly, the extraction behavior of TB24C8-2 (**13**) resembled that of the monobenzo-24-crown-8 (**9**) rather than that of its structural isomer TB24C8-1 (**11**).

**Reagents.** Alkali metal picrates were obtained as described elsewhere<sup>21</sup> and stored in the cool, dark place. *Caution! Metal picrates are potential explosive hazards which are sensitive to heat, friction, or impact.*

Benzo group-containing CEs **1**, **4**, **7**, and **10** and dicyclohexano-CE **5** (a mixture of cis-syn-cis and cis-anti-cis isomers) were commercially available compounds. Monobenzo-CE **9** was obtained by the literature procedure.<sup>22</sup> For the preparation of **14** and **15**, improved procedures (refs 13 and 23, respectively) were applied. Earlier reported<sup>2</sup> **2** and the polybenzo-CES **3**, **8**, **11**, and **12**, as well as **6**,<sup>24</sup> were obtained in enhanced yields by reactions of the appropriate bisphenol and poly-(ethylene glycol) dimesylate with Cs<sub>2</sub>CO<sub>3</sub> in CH<sub>3</sub>CN. Similarly, the synthesis of a new isomer of tribenzo-24-crown-8 **13** was achieved in 75% yield from 1,2-bis(2'-hydroxyphenoxy)ethane<sup>25</sup> and 1,2-bis(5-hydroxy-3-oxapentylloxy)benzene dimesylate (the detailed procedure will be published later.) **13**: mp 120–122 °C; IR (deposit from CHCl<sub>3</sub> onto a NaCl plate)  $\nu$  1255 and 1124 (C–O) cm<sup>-1</sup>; <sup>1</sup>H NMR (300 MHz, CDCl<sub>3</sub>)  $\delta$  3.89–3.96 (m, 8H), 4.09–4.12 (m, 4H), 4.18–4.21 (m, 4H), 4.37 (s, 4H), 6.85–6.96 (m, 12H); <sup>13</sup>C NMR (75 MHz, CDCl<sub>3</sub>)  $\delta$  67.82, 69.57, 69.91, 70.10, 70.34, 114.62, 114.68, 116.61, 121.55, 121.68, 122.03, 148.92, 149.10, 149.40. Anal. Calcd for C<sub>28</sub>H<sub>32</sub>O<sub>8</sub>: C, 67.73; H, 6.50. Found: C, 67.52; H, 6.46.

**Procedures. (a) Analytical.** Competitive alkali metal picrate extraction was conducted with an aqueous solution containing Li<sup>+</sup>, Na<sup>+</sup>, K<sup>+</sup>, Rb<sup>+</sup>, and Cs<sup>+</sup> (1.0 mM in each, together with 5.0 mM of each sulfate as a spike) and a 1.0 mM CHCl<sub>3</sub> solution of the CE. Competitive alkali metal iodide extraction was performed with an aqueous solution which was 0.50 M in each of the alkali metal iodides and a 10.0 mM solution of the CE in CHCl<sub>3</sub>. After back-extraction of the alkali metal salts from the separated CHCl<sub>3</sub> layer into deionized H<sub>2</sub>O (at least three consecutive stripping treatments were performed to ensure the completeness of back-extraction), the metal ion concentrations in the combined aqueous stripping solutions were determined by ion chromatography. Three independent extraction experiments were conducted for each combination of CE and alkali metal salt. Relative to the other alkali metal ions extracted, the amount of Li<sup>+</sup> was too small for accurate determination. Separation factors,  $\alpha_{M_1, M_2}$ ,<sup>11</sup> were calculated from the corresponding distribution ratio values,  $D_{M_1}/D_{M_2}$ .

After the MPic extraction with **3** as well as MPic and MI extraction with **12** had been completed and the phases separated, a precipitate formed in the organic layer. After filtering, the organic layer was stripped and analyzed as described above. The precipitate was washed with chloroform, dried in vacuo, and analyzed for alkali metal content as described elsewhere.<sup>13</sup>

**(b) General Procedure for Preparation of the Alkali Metal Picrate Complexes with the CEs.** A 30.0 mM solution of the CE in CHCl<sub>3</sub> was stirred magnetically with an excess of solid MPic for 24 h. The mixture was filtered and the separated solid was washed on the filter with boiling CHCl<sub>3</sub>. The combined CHCl<sub>3</sub> filtrate and washing were evaporated in vacuo and the resultant solid was recrystallized from CH<sub>2</sub>Cl<sub>2</sub>–CH<sub>3</sub>OH (5:1).

For the <sup>1</sup>H NMR spectral measurement, a solution of the MPic–CE complex was prepared by stirring a 30.0 mM solution of the CE in CDCl<sub>3</sub> (used without drying) with an excess of the solid MPic for 24 h. The mixture was filtered and its <sup>1</sup>H NMR spectrum was recorded at 297 K. For probing the effect of concentration on  $\delta_{H-Pic}$ , solutions of the M<sup>+</sup>LPic<sup>-</sup> were prepared by sequential dilutions with CDCl<sub>3</sub> of 150 mM solutions of these complexes in CDCl<sub>3</sub>.

(21) Coplan, M. A.; Fuoss, R. M. *J. Phys. Chem.* **1964**, *68*, 1177–1180.

(22) Zhilina, Z. I.; Mel'nik, V. I.; Andronati, S. A.; Abramovich, A. E. *J. Org. Chem. USSR (Translation of Zh. Org. Khim.)* **1989**, *25*, 957–963 (Eng).

(23) Talanov, V. S.; Bartsch, R. A. *Synth. Commun.* **1999**, *29*, 3555–3560.

(24) Keulen, B. J.; Kellogg, R. M.; Piepers, O. *J. Chem. Soc., Chem. Commun.* **1979**, 285–286. Reinhoudt, D. N.; de Jong, F.; Tomassen, H. P. M. *Tetrahedron Lett.* **1979**, 2067–2068.

(25) Harrison, B. T. *J. Chem. Soc., Chem. Commun.* **1969**, 616–617.

### X-ray Data Collection, Structure Determination, and Refinement.

A single crystal obtained by slow air evaporation of CH<sub>2</sub>Cl<sub>2</sub>–CH<sub>3</sub>OH solutions of the complex was mounted on a fiber and transferred to the goniometer of a Siemens CCD area detector-equipped platform diffractometer. A stream of cold nitrogen gas was used to cool the crystal to –100 °C during data collection. The data collection, reduction, absorption correction, and structure solution and refinement were carried out with the Siemens software products SMART, SAINT, SADABS, and SHELXTL, respectively. Unit cell data were determined by a global refinement of several thousand reflections within the data collection range. The space group was determined using systematic absences and subsequent solution and successful refinement of the structure (to distinguish between centric and acentric choices). Refinement was full-matrix, least-squares of  $F^2$ . **KPic–2**: KPic·**2**, C<sub>26</sub>H<sub>26</sub>KN<sub>3</sub>O<sub>13</sub>,  $M = 627.60$ , yellow parallelepiped, triclinic  $P1$ ,  $a = 7.5552(6)$  Å,  $b = 12.8200(9)$  Å,  $c = 14.6982(10)$  Å,  $\alpha = 84.318(2)^\circ$ ,  $\beta = 76.749(2)^\circ$ ,  $\gamma = 88.233(2)^\circ$ ,  $Z = 2$ , final  $R [I > 2\sigma(I)] R1 = 0.0497$ ,  $wR2 = 0.0947$ ,  $GOF = 0.978$ . **RbPic–2**: RbPic·**2**, C<sub>46</sub>H<sub>50</sub>N<sub>3</sub>O<sub>19</sub>Rb,  $M = 1034.36$ , yellow fragment, triclinic  $P1$ ,  $a = 12.9339(11)$  Å,  $b = 13.4891(11)$  Å,  $c = 15.9603$  Å,  $\alpha = 101.375(2)^\circ$ ,  $\beta = 102.532(2)^\circ$ ,  $\gamma = 113.005(2)^\circ$ ,  $Z = 2$ , final  $R [I > 2\sigma(I)] R1 = 0.0738$ ,  $wR2 = 0.2075$ ,  $GOF = 1.031$ . **KPic–3**: KPic·**3**, C<sub>30</sub>H<sub>26</sub>KN<sub>3</sub>O<sub>13</sub>,  $M = 675.65$ , yellow fragment, triclinic  $P1$ ,  $a = 7.2884(5)$  Å,  $b = 14.0914(6)$  Å,  $c = 14.1719(9)$  Å,  $\alpha = 90.962(3)^\circ$ ,  $\beta = 95.945(2)^\circ$ ,  $\gamma = 96.982(3)^\circ$ ,  $Z = 2$ , final  $R [I > 2\sigma(I)] R1 = 0.0997$ ,  $wR2 = 0.1714$ ,  $GOF = 0.944$ . **KPic–4**: KPic·**4**·H<sub>2</sub>O, C<sub>26</sub>H<sub>28</sub>KN<sub>3</sub>O<sub>14</sub>,  $M = 645.61$ , yellow parallelepiped, triclinic  $P1$ ,  $a = 7.5876(2)$  Å,  $b = 13.3035(4)$  Å,  $c = 14.4104(3)$  Å,  $\alpha = 92.533(1)^\circ$ ,  $\beta = 103.599(1)^\circ$ ,  $\gamma = 92.467(1)^\circ$ ,  $Z = 2$ , final  $R [I > 2\sigma(I)] R1 = 0.0420$ ,  $wR2 = 0.0934$ ,  $GOF = 1.000$ . **RbPic–4**: (RbPic·**4**)<sub>2</sub>,  $M = 1347.94$ , colorless parallelepiped, orthorhombic  $Pmm2_1$ ,  $a = 25.9701(1)$  Å,  $b = 12.0711(2)$  Å,  $c = 8.9440(1)$  Å,  $\alpha = 90^\circ$ ,  $\beta = 90^\circ$ ,  $\gamma = 90^\circ$ ,  $Z = 2$ , final  $R [I > 2\sigma(I)] R1 = 0.0428$ ,  $wR2 = 0.1093$ ,  $GOF = 1.070$ . **RbPic–8**: RbPic·**8**, C<sub>32</sub>H<sub>30</sub>N<sub>3</sub>O<sub>14</sub>Rb,  $M = 766.06$ , yellow fragment, triclinic  $P1$ ,  $a = 12.1544(3)$  Å,  $b = 12.6001(3)$  Å,  $c = 12.9493(3)$  Å,  $\alpha = 61.601(1)^\circ$ ,  $\beta = 68.438(1)^\circ$ ,  $\gamma = 77.943(1)^\circ$ ,  $Z = 2$ , final  $R [I > 2\sigma(I)] R1 = 0.0609$ ,  $wR2 = 0.1482$ ,  $GOF = 0.792$ . **CsPic–11**: CsPic·**11**·0.5CH<sub>3</sub>OH, C<sub>34.5</sub>H<sub>36</sub>CsN<sub>3</sub>O<sub>15.5</sub>,  $M = 873.57$ , yellow fragment, triclinic  $P1$ ,  $a = 13.2377(6)$  Å,  $b = 16.6041(7)$  Å,  $c = 18.4215(8)$  Å,  $\alpha = 104.519(1)^\circ$ ,  $\beta = 102.029(1)^\circ$ ,  $\gamma = 100.466(2)^\circ$ ,  $Z = 4$ , final  $R [I > 2\sigma(I)] R1 = 0.0705$ ,  $wR2 = 0.1421$ ,  $GOF = 0.853$ . **RbPic–12**: RbPic·**12**·1.5CH<sub>2</sub>Cl<sub>2</sub>, C<sub>39.25</sub>H<sub>36.5</sub>Cl<sub>2.5</sub>N<sub>3</sub>O<sub>15</sub>Rb,  $M = 964.31$ , yellow parallelepiped, triclinic  $P1$ ,  $a = 13.5135(1)$  Å,  $b = 16.8163(5)$  Å,  $c = 19.3287(6)$  Å,  $\alpha = 84.230(1)^\circ$ ,  $\beta = 81.716(1)^\circ$ ,  $\gamma = 76.921(1)^\circ$ ,  $Z = 4$ , final  $R [I > 2\sigma(I)] R1 = 0.0899$ ,  $wR2 = 0.2063$ ,  $GOF = 0.971$ . **CsPic–12**: CsPic·**12**·1.5CH<sub>2</sub>Cl<sub>2</sub>, C<sub>39.25</sub>H<sub>36.5</sub>Cl<sub>2.5</sub>N<sub>3</sub>O<sub>15</sub>Cs,  $M = 1011.75$ , yellow parallelepiped, triclinic  $P1$ ,  $a = 13.5085(2)$  Å,  $b = 16.8244(3)$  Å,  $c = 19.2714(1)$  Å,  $\alpha = 84.283(1)^\circ$ ,  $\beta = 81.835(1)^\circ$ ,  $\gamma = 76.771(1)^\circ$ ,  $Z = 4$ , final  $R [I > 2\sigma(I)] R1 = 0.0411$ ,  $wR2 = 0.0873$ ,  $GOF = 1.030$ .

**Acknowledgment.** This research was supported by Grant D-775 from the Robert A. Welch Foundation. The authors appreciate valuable discussions from Professor Georges Wipff of the Institut de Chimie, Strasbourg, France, and Professor Konstantin B. Yatsimirskii of the L. V. Pisarshevskii Institute of Physical Chemistry of NAS of Ukraine, Kiev, Ukraine.

**Supporting Information Available:** A thermal ellipsoid figure, a table of required crystal data and experimental details, a table of positional and thermal parameters, a detailed discussion for each reported structure, two tables of separation factor values for competitive extractions of alkali metal picrates and iodides with crown ethers **1–13**, and an explanation of the expected linearity of plots ( $\alpha_{M_1, M_2}$ )<sub>Pic</sub> vs ( $\alpha_{M_1, M_2}$ )<sub>I</sub> (PDF). This material is available free of charge via the Internet at <http://pubs.acs.org>.